J. D. HALAJIAN and H. B. HALLOCK
Grumman Aircraft Engineering Corp,
Bethpage, N.Y,

Uses of Temporal Data in Remote Sensing

The potential of complementing pictorial data with the study of the time behavior of quantified radiation from a target element is explored. To date, most studies of remote surfaces have been severely restricted to visual impressions from images, particularly in the visible wavelengths. Temporal analysis of the quantity, polarization, and spectral distribution of the electromagnetic flux from each element during a transient cycle promises information beyond the resolution of the viewing system.

Laboratory analogs and theoretical models are used to illustrate the way that lunar photometric, polarimetric, and radiometric data can be correlated with roughness, porosity, bearing strength, internal heat sources, etc. Surveyor data are used in order to verify the correlations and to resolve some ambiguities. It is shown that Earth-based, high-resolution observations of the diurnal behavior of the lunar surface at optical and infrared wavelengths could supplement Orbiter photographs and lead to the discovery of suitable landing sites and/or prime targets of exploration. The importance of prereconnaissance diagnostic research and postreconnaissance ground truth measurements as integral parts of a remote sensing strategy is stressed.

INTRODUCTION

At the present time the consensus is that orbital reconnaissance of terrestrial and extra-terrestrial surfaces should be a major objective of the post-Apollo period. It is believed that high-resolution, multisensor data on a synoptic scale will help mission planners and experimenters in selecting prime targets of exploration, in laying out optimum geologic traverses, and in devising key surface measurements. In practice, this strategy will be only as effective as our ability to extract useful information from the raw remote sensor data with a minimum of ambiguity. Certainly, the vast quantity and spectral variety of orbital data will necessitate improved methods of data collection, processing, and interpretation. However, a survey of the recent literature of remote sensing shows a greater preoccupation with sensor development than with data diagnosis. While both tasks are equally important, this paper will primarily concentrate on the latter and will focus atten-

tion on an area of remote sensing concerning what are called "temporal data" in this report. Such data are simply measurements of electromagnetic radiation as a function of time, as compared, for example, with pictorial data which essentially represent the spatial distribution of the same radiation at any wavelength but at a given instant of time.

Changes in brightness and temperature of a planetary surface during a day-and-night cycle are examples of temporal data. An attempt will be made to illustrate by means of experiments, theoretical models, and qualitative discussions the way in which such data could supplement purely pictorial information. Another of the present paper is to stress the importance of prereconnaissance homework in data interpretation as an integral part of the overall strategy of remote sensing, particularly from an orbit. This preparatory analysis may well determine whether the data should be acquired in the first place and, if so, how they should be acquired in terms of choice of sensor

or sensors, time of observation, geometry of viewing, etc.

TEMPORAL DATA AND THE OVERALL PICTURE IN REMOTE SENSING

Electromagnetic energy measured by remote means may be classified into pictorial, spectral, and temporal data, the designation depending on whether such data represent the distribution in space, the distribution in wavelength, or the variation with time of the energy, respectively.

Our concept of temporal data has its origin in the study of lunar astronomical data. At optical wavelengths, the temporal nature of these data emerges from the dependence of brightness on the direction of incidence (and viewing) during an insolation cycle. This cycle could also be a satellite orbital period, a season, or other natural event or even a manmade event. At infrared wavelengths, in addition to directional factors affecting radiance, cyclic heating and cooling contribute to the temporal aspect. In terrestrial remote sensing it is common to catalog into time-oriented interpretation keys the infrared response of surfaces under various meteorological conditions during a diurnal cycle. This is an example of effective utilization of temporal data. It is not an essential condition to this utilization that continuous observations over a complete temporal cycle be accomplished in the actual reconnaissance of the surface. More frequently it is expedient to match discontinuously recorded responses with an interpretation key which itself represents continuity of observation over a temporal cycle. In other words, the field data could represent a few points on the complete temporal function of known models.

The need for similar interpretation keys for the optical photometric and polarimetric responses is not equally obvious because temporal changes at optical wavelengths are less dramatic than those at the infrared ones, but nevertheless these changes could be of diagnostic value provided that they are measured with high fidelity. Extensive time-oriented interpretation keys at optical wavelengths eventually may prove very valuable as sensor gray-tone

resolution is improved. Consequently, advantage can be taken from the time-varying parameters to extract more information than would appear possible by the use of pictorial interpretation only. The advantages can be realized only by very accurate preservation of gray-tone values. This, however, would involve improvement in sensor capability which is beyond the scope of the present report.

To date, most studies of remote surfaces have been restricted to visual impressions from photographs. A concept that deserves emphasis is the idea that photographs are necessary as visual, synoptic records of the size and location of surface features or gray tones, but they are not sufficient in all cases for a positive identification of these features. This inadequacy stems from the fact that many factors, such as albedo, slope, and shadowing by unresolved features, could contribute to the gray-tone values. It is not always possible to disentangle these factors without a quantitative analysis of the spectral and temporal signatures of the features in question. At longer-than-visual wavelengths there are additional factors which may cause ambiguities, such as the mechanical, thermal, and electrical properties of the surface layers, all of which tend to modify pictorial gray tones.

Generally, the coarser the resolution of imagery, the greater is the need for quantitative data on an object's spectral and temporal tone signatures and the less is the reliance that can be placed on the object's spatial configuration. Since spectral and temporal tone signatures of rocks, soils, and vegetation types quite often may indicate their composition and structure, tone signatures assume considerable importance in the interpretation of many features that are of interest in Earth resources and planetary exploration.

Those data usually referred to as photometric, polarimetric, and radiometric in the lunar literature are classic examples of temporal data. These data have received considerable attention in recent years, but more as isolated areas of scientific inquiry than as contributory clues to the overall picture in remote sensing. Figure 1 shows the major components and subcomponents of this picture. In the three-step process outlined, the first two steps
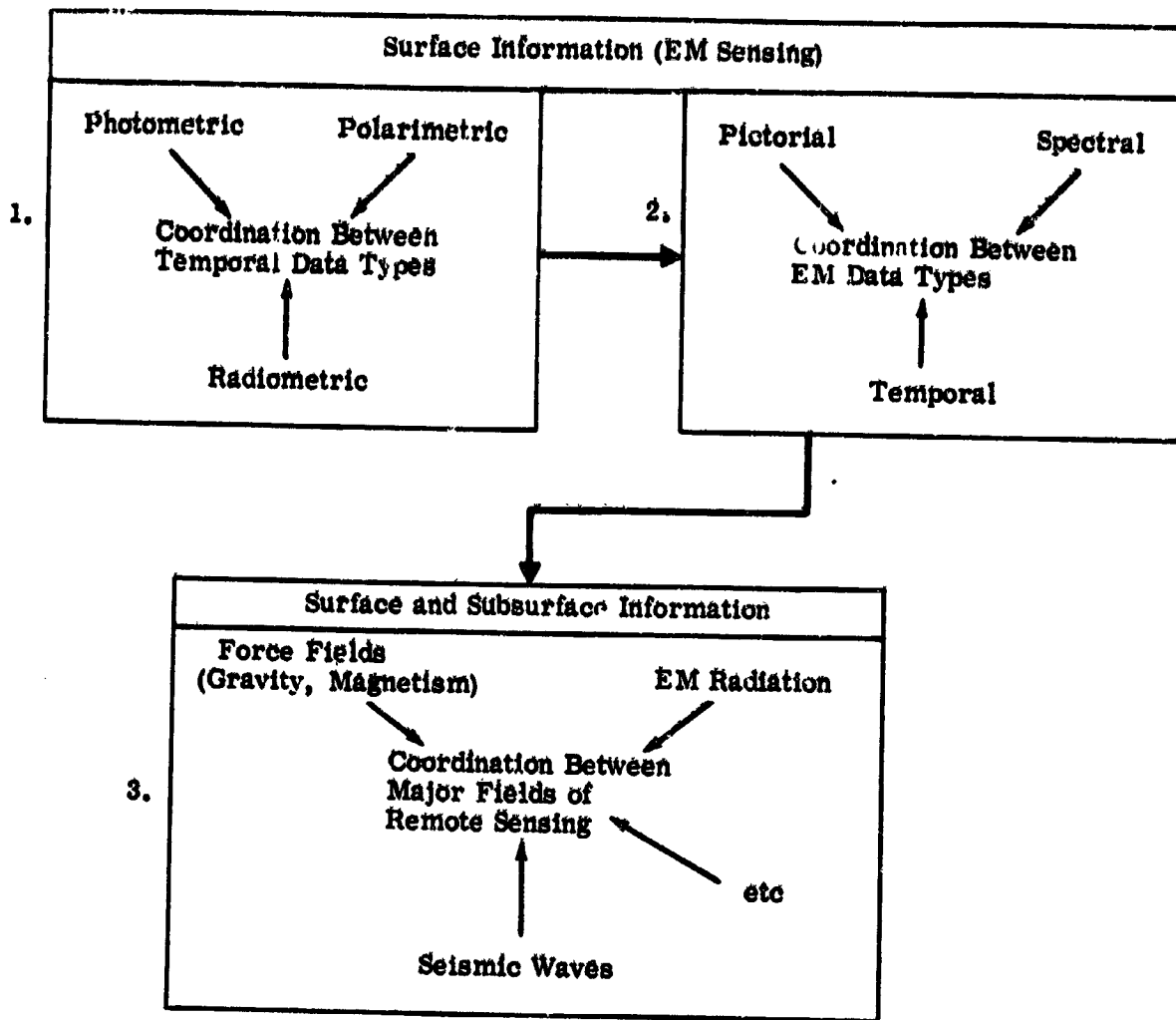
Figure 1.—Steps in coordinating temporal and other forms of remote sensor data.

involve electromagnetic (EM) methods of sensing. These methods provide information about the surface and near-surface material. In the first step temporal data are cross-correlated at visible and longer wavelengths. In the second step this information is used to supplement pictorial and spectral data. Step 3 gives a third dimension to the picture; it consists of combining the surface information obtained in steps 1 and 2 with subsurface data obtained by means of seismic and force-field surveys.

Since few temporal data on terrestrial surfaces currently exist, the lunar astronomical and Surveyor data are used to illustrate the techniques of cross-correlating temporal and pictorial data as outlined in steps 1 and 2 of figure 1. Spectral data (also in step 2) are not used, since such data and their correlation with material composition have been extensively investigated in the laboratory and the field by Adams (ref. 1), Hovis (ref. 2), Lyon (ref. 3), and others. As to step 3, there are no case studies at our disposal to show how it may be implemented. However, it is reasonable to predict that extraterrestrial targets, which will be explored by onsite geophysical techniques, will be selected by sifting orbital data obtained by electromagnetic means.

TYPES OF LUNAR TEMPORAL DATA

Figure 2 shows three well-known, typical "signatures" of the lunar surface. The curves are qualitative in nature and are meant to show general trends with time. The curve in figure 2(a) is known as the photometric function. It represents the change in the visible brightness of the lunar surface between sunrise and sunset (ref. 4). It is characterized by rapid increase in brightness at full moon and a continuous drop in brightness after full moon at all phase and viewing angles (phase angle is the angle between light rays incident on the Moon and the reflected rays as seen by an observer on Earth). This signature is called a backscattering type and is indicative of a rough surface.

A similar measurement of the percent polarization of the visible brightness (ref. 5) results in the curve shown in figure 2(b). It is characterized by negative polarization (about 1.5 percent) at small phase angles near full moon, a

reversal to positive polarization at phase angles of about 23°, and a maximum positive polarization at large phase angles generally not exceeding 20 percent. The counterpart of the photometric and polarimetric curves at near-infrared wavelengths (0.8 to 3μ) is not known, hence the question mark in figure 2(c).

Radiation from the lunar surface in the infrared (mostly 8 to 14μ) has been measured by numerous investigators (refs. 6, 7, and 8) both during a lunation and an eclipse. The results can be represented as effective surface temperature variation with time, as shown in figure 2(d). Notice that the daytime portion of the temperature curve, unlike that of the photometric curve, is convex, and the nighttime or eclipse portion is nearly a straight line.

By assuming that the curves of figure 2 represent the norm for the lunar surface, we shall discuss successively the manner in which these temporal signatures could deviate from the norm and what these deviations may
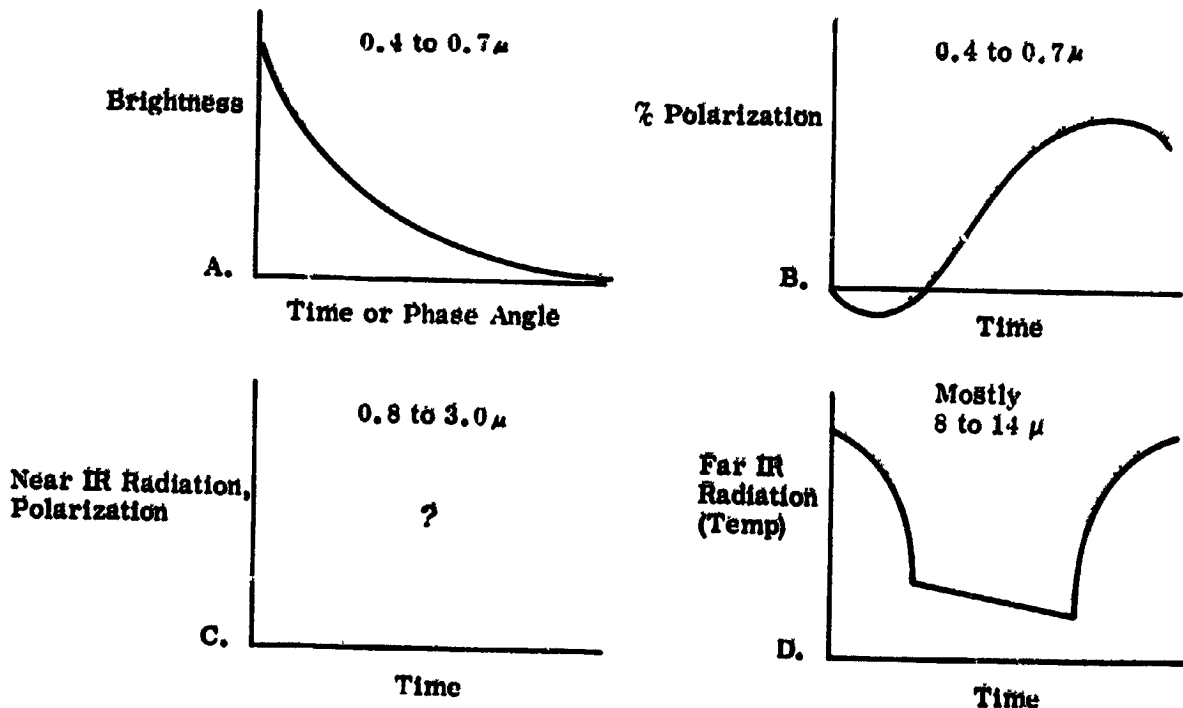

Figure 2.—Types of lunar temporal signatures.

(a) Photometric curve, 0.4 to 0.7 μ.
(b) Polarimetric curve, 0.4 to 0.7 μ.
(c) Polarimetric curve at 0.8 to 3.0 μ.
(d) Temperature curve, 8 to 14 μ.

mean in terms of the physical properties of the terrain.

PHOTOMETRIC ANOMALIES AND THEIR MEANING

Correlation Between Surface Roughness and Shape of Photometric Curve

There are a number of factors that perturb the lunar photometric curve. The most important of these factors is shadowing. Indeed, it is commonly recognized that a cause-and-effect relationship exists between surface roughness and the shape of the photometric curve. It has been believed, for instance, that a complex microstructure is primarily responsible for the peculiar photometric properties of the lunar surface. However, no attempts have been made, to our knowledge, to isolate the effect of this microstructure on the photometric signature and, in addition, to determine whether information on large-scale structures beyond the resolution of the viewing system could be extracted from this signature. We now propose to investigate this problem.

First, to appreciate why photometric data can supplement photographs in providing information about roughness beyond the resolution of the particular viewing system that is being used, it is necessary to recall some essential characteristics of photometry and photography. A photograph is a qualitative record of the spatial distribution of brightness. The same record properly calibrated and controlled can become the basis for the quantitative study of this distribution, known as photometry. The expression "lunar photometry" is the study of the directional properties of reflected sunlight and as such it may be considered to be the temporal extension of photography. It consists of the measurement of the total flux from each or all resolution elements in the field of view and of the change with time of this flux during a complete insolation. Thus, one may conceive of the photometric curve as a motion picture of shadowing and of a photograph as a frame in that picture. Photographic observations differentiate between gray tones within the resolution capability of the viewing system.

Photometric reduction integrates all these effects over any chosen field of view within the photograph. If the integration is done on one element of resolution and expressed as a function of phase angle, then the resulting photometric curve reveals the temporal behavior of shadows cast by features smaller than the resolution of the system. Thus, it is in the quantitative analysis of the temporal and directional changes of the reflected flux from a discrete area that photometry can complement photography in the assessment of unresolved roughness.

The most accurate photometric data on the lunar surface presently are taken with photoelectric sensors of excellent linearity and calibration rather than through direct film photography. The resolution of a photoelectric system usually is taken to be the field of view of any one sensor element. Unresolved shadows would fall within this field.

In figure 2(a) the following features of the photometric curve are selected for their diagnostic values: (1) the area under the normalized curve, (2) the slope of the curve near its peak (i.e., the region of opposition), and (3) the curvature and ordinate value of the tail end of the curve (i.e., the region of specularity at oblique viewing). We propose that these features are clues to terrain properties which will now be discussed.

Total Roughness

Total roughness is defined as an index of the integrated effect of all unresolved shadow-casting protrusions in the field of view, which could include features ranging from particles of dust to mountains. For a given viewing angle, the area under the normalized backscattering photometric curve is a function of the cumulative shadowing effect of all these irregularities. This correlation of photometry with surface structure has been demonstrated satisfactorily in numerous experiments in which specimens ranging from solid rocks to very rough, dendritic sea corals were examined with a photometer having a large area-viewing capability (ref. 9).

A slight variation of previously reported

8 cm

Aa Lava, Albedo = 8%

Viewing Angle = 60°

Smooth Anomaly
(Area 1 in Photo)

Average Moon

Whole
Specimen

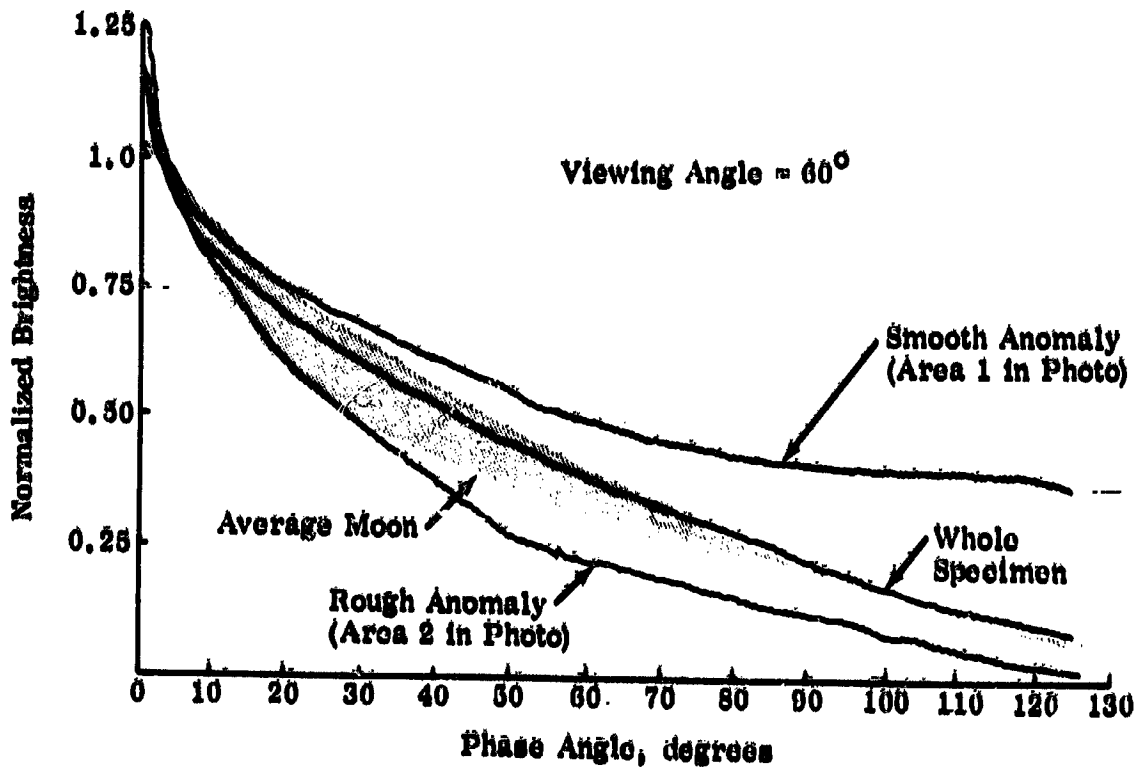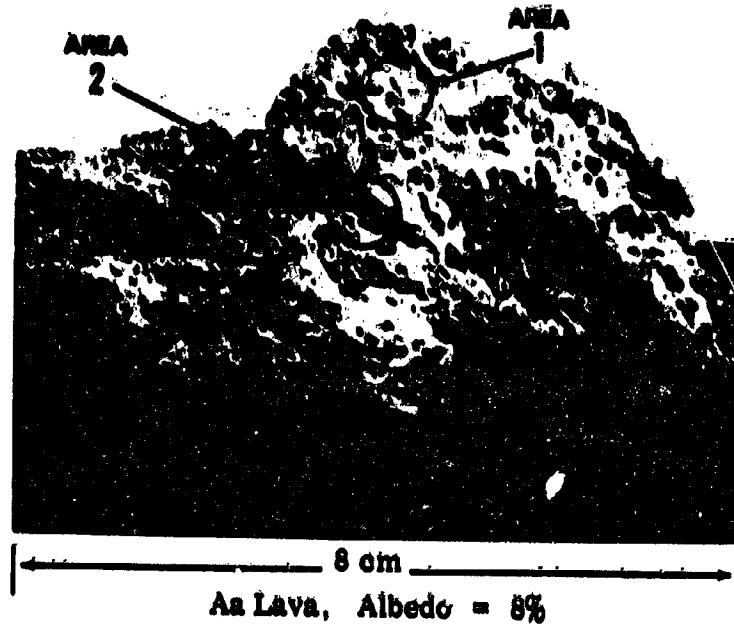Rough Anomaly
(Area 2 in Photo)

Phase Angle, degrees

FIGURE 3.—Correlation of total roughness with area under photometric curve.

experiments is shown in figure 3 for the purpose of illustrating the way, in telescopic observation of the Moon, that photometric anomalies could be detected by improving the spatial resolution of the measurements. The specimen selected for this experiment is a dark vesicular lava (8 percent albedo) containing numerous cracks and a few isolated smooth anomalies located between the large irregularities. The improvement in spatial resolution is accomplished first by viewing the whole specimen with a large, 1.5° field stop (this corresponds to an area 8 centimeters in diameter on the sample table) and then by reducing the field stop to 0.3° and focusing the photometer successively on one of the smooth and rough anomalies.

In figure 3 the coarse-resolution view gives a good photometric match with the lunar standard (shaded band), but the fine-resolution view of the smooth and rough spots brings out the anomalies. It is clear that the area under the anomaly curves is larger or smaller than the area under the curve representing the whole specimen and that there is a trend of increasing area with decreasing roughness.

The fact that the relative roughness of two or more regions can be predicted in this manner is considered quite favorable to the photometric technique for remote sensing of roughness beyond the imaging resolution of the optical system. Conceivably many photometric anomalies could exist on the Moon that have not been discovered but which could be detected and located by telescopic instrumentation of high resolution and gray-tone accuracy.

The area rule is valid for most rough, textured surfaces encountered in nature, such as rocks, soils, and vegetation, when the specular component of brightness is quite subdued compared with the backscatter component. This case should be the rule rather than the exception for the Moon. If there are exceptions, their discovery will be significant.

Microstructure

Microstructure is defined as the random, small-scale roughness that characterizes the texture or surface porosity of a material. The random orientation of the microelements (that

is, random with respect to the gravity vector) makes it possible to distinguish them photometrically from the macroelements which, by our definition, are predominantly oriented by gravity. It is now proposed that the slope of the photometric curve in the region of opposition (between phase angles of 0° to 10°) is an index of microstructure. A surface like the Moon as a whole which exhibits a sharp brightness peak of 0° phase angle, regardless of the direction of viewing, necessarily must be covered with randomly oriented elements interspaced with deep, and possibly interconnected, cavities. It follows that the shadow-casting elements in the opposition region must be small, of the order of centimeters and smaller, in order to maintain their random orientation in a gravity field. As a rule, the steeper the slope of the curve in the opposition region, the rougher is the microstructure.

Macrostructure

Large topographic features such as boulders and craterlets (or mountains and craters, the size depending on the size of the field of view) are categorized as macrostructure by virtue of the orientation of their height (or depth) along the gravity vector. Such features cast shadows that become visible to an observer only when the Sun is on the opposite side of the local vertical, such as early in the morning or late in the afternoon. These shadows largely are responsible for depressing the tail end of the photometric curve. The microstructure has little or no effect on this part of the curve, because the small cavities are saturated with shadows at the large phase angles and a microelement is, by definition, too small to over-shadow a photometrically significant number of other microelements. In the absence of large-scale roughness, the photometric curve is most likely to exhibit a "bulge" or a second brightness peak at the specular angle in oblique viewing.

It should not be surprising that lunar areas exhibiting a second brightness peak have not been discovered. In telescopic observation of the Moon, the field of view usually is sufficiently large to include numerous topographic features

which cast long shadows at large phase angles and, hence, depress the tail end of the photometric curve. The possibility of discovering optically enhanced (i.e., smooth) areas on the Moon should not be discounted in view of significant improvements that can be made in the quantity and quality of the existing telescopic data.

The following experiment was performed in order to demonstrate the aforementioned proposed relationship between scale of roughness and shape of photometric curve. The photometry of a microrough surface with and without macroroughness was measured at normal and 60° off-normal viewing angles, as shown in

figure 4. The microrough surface was simulated by means of a dark, synthetic urethane foam of low albedo (6 percent). This material was selected because of its very high porosity (97 percent) and, consequently, because of its promise of an exaggerated backscatter response in the opposition region as predicted by our hypothesis. Macroroughness was simulated by placing a few centimeter size microporous volcanic cinders on the foam. An area 8 centimeters in diameter was sampled by the photometer. The output of the xy recorder registering the photometric signature was normalized with the lunar standard (shaded band in fig. 4) at a 4° phase angle. The brightness in the opposi-
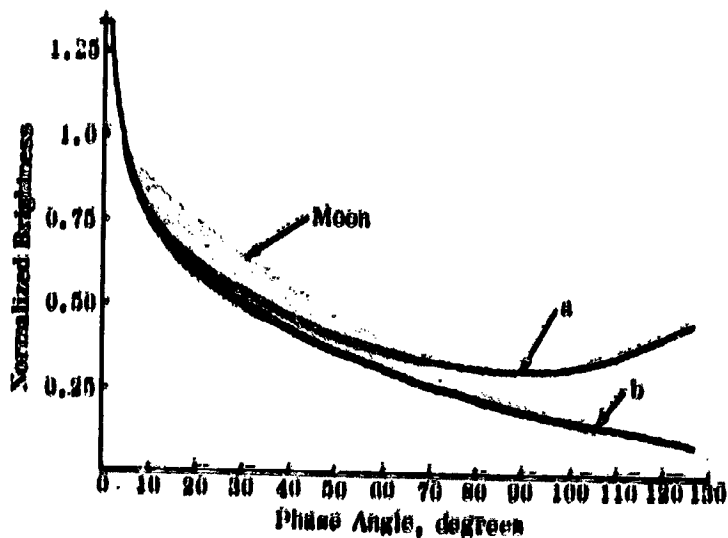

A.

B.
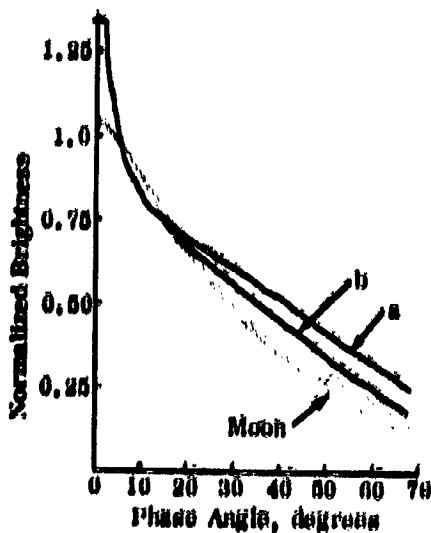
C.

D.

FIGURE 4.—Correlation of microroughness and macroroughness with components of photometric curve.
(a) Microrough surface, urethane foam; porosity, 97 percent; albedo, 6 percent; view angle, 60°.
(b) Microrough and macrorough surface, foam plus volcanic cinders; albedo, 6 percent; view angle, 60°.
(c) View angle, 0°.
(d) View angle, 60°.

this region was measured by means of a beam splitter placed between photometer and sample. The beam splitter was sufficiently long in the plane of the intensity equator to enable brightness measurements between phase angles of −7° to 12° to be made.

As anticipated, the foam, because of its extremely complex microstructure, exhibited a slope in the opposition region that was steeper than anything previously seen. In all cases, the upsurge of brightness was so intense that the output went beyond the field of the recorder, as can be seen in figure 4. Latest lunar data reported by Gehrels et al. (ref. 10) indicate an opposition effect somewhere between the foam curve and the lunar standard in figure 4. From this it may be inferred that the foam is more porous than is the lunar surface.

Notice also in figure 4 that the foam without the volcanic cinders exhibits a second brightness peak toward the specular direction (phase angle 120°), but the addition of the volcanic cinders lowers the brightness to the level of the lunar norm. This experiment also showed that the tail end of the curve is more sensitive to microroughness at oblique viewing than at normal viewing. Although viewing at oblique angles entails some loss of spatial resolution, we believe that the superior diagnostic value of the photometric curve at oblique viewing more than compensates for this loss.

In conclusion, it seems possible to rate the relative roughness of discrete regions by comparing the time integral of their brightness over an insolation cycle (this is the area under the photometric curve). It also seems possible to infer surface texture and large-scale roughness below the resolution of the viewing system by studying the actual shape of the photometric curve.

Photometry as an Aid in Photographic Interpretation

It is often necessary to study the temporal behavior of photographic features in order to determine whether the apparent diversity of gray tones is caused by differences of composition, of structure, or of both.

The recent controversy concerning the nature of the dark ejecta observed around the Surveyor footprints is a case in point. This problem was discussed in a recent publication and it was shown by means of simulation experiments how accurate data on the albedo and photometry of the gray tones in question could settle the issue (ref. 11). Another example is the case of the lunar rays which, as is well known, are conspicuous at full moon but tend to disappear and blend into the background at large phase angles. It appears that this peculiar photometric behavior indicates that the rays differ from their surroundings in both albedo and structure. This proposition is based on the following reasoning. The brightness of a surface at 0° phase angle depends only on its normal albedo, but at phase angles other than 0° this brightness is attenuated by the extent of shadowing, hence by the roughness or porosity of the surface. Accordingly, two areas of unequal normal albedo when viewed at a large phase angle could conceivably register the same brightness or gray tone on a photograph if the lighter area (in terms of normal albedo) is rougher or more porous than is the darker area. This behavior is indeed exhibited by the lunar rays. Hence, it is sufficient to postulate that the ray areas are inherently lighter and rougher than their surroundings in order to account for this peculiar behavior. The rays cannot be discriminated from their background at large phase angles, because their inherently higher reflectivity is attenuated by a large number of shadows cast by features that are usually too small to be resolved by the viewing system.

An experiment was performed in which the above-postulated properties were simulated in the following manner: A layer of dark, backscattering volcanic powder (particle size 38 to 88 micron and normal albedo 14 percent) was deposited on a flat board and firmly tamped; then a lighter powder (normal albedo 16 percent, same particle size) was loosely sifted over this layer through a template incorporating a ray pattern. Figure 5(a) shows a photograph of the simulated rays taken under ambient, non-collimated lighting. Figures 5(b) and 5(c) show
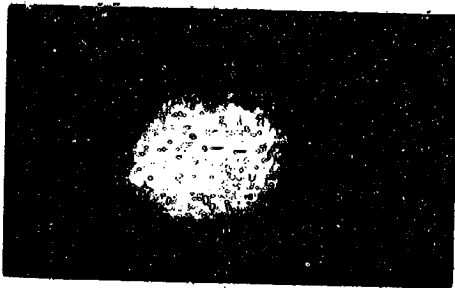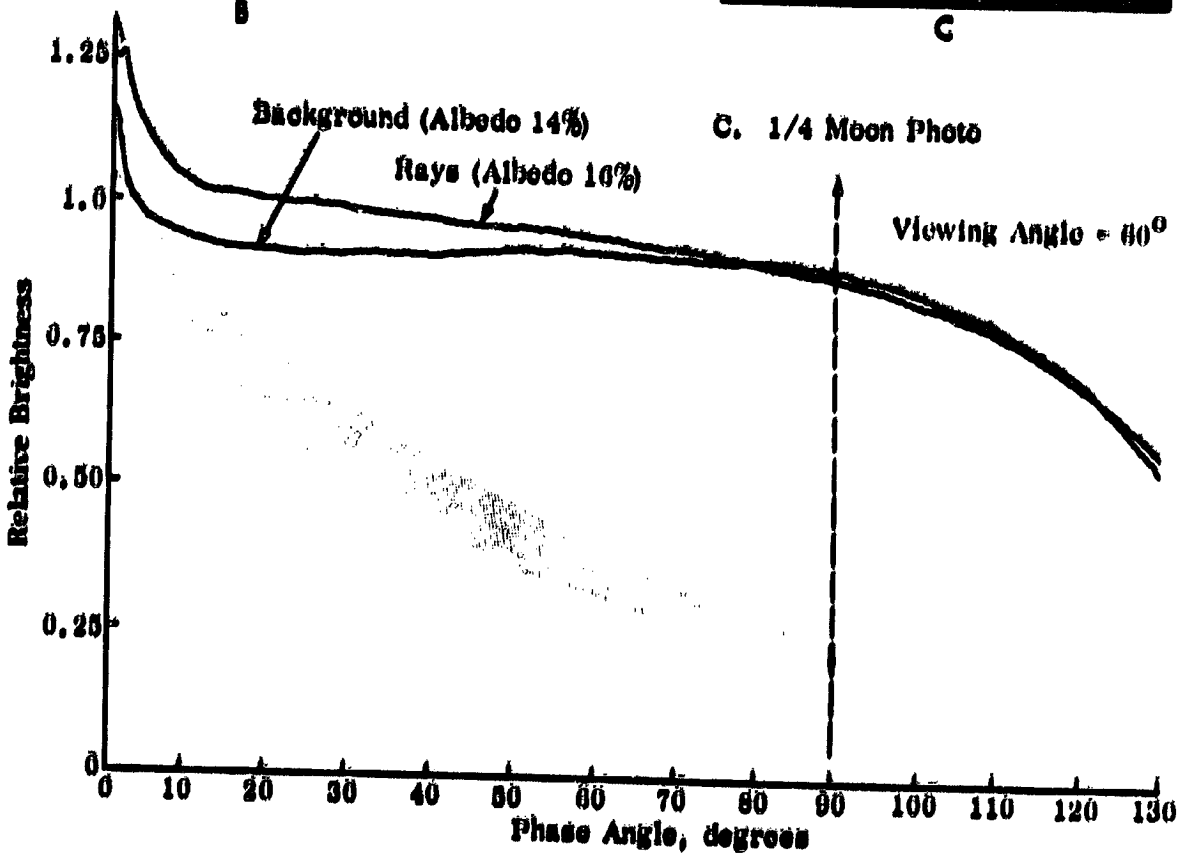
Figure 5. Photometric behavior of simulated lunar rays.
(a) Photograph of simulated rays under ambient, noncollimated lighting.
(b) Photograph of scene in figure 5(a) under collimated lighting at 0° phase angle.
(c) Photograph of scene in figure 5(a) under collimated lighting at 60° phase angle.
(d) Photometric curves of the rays.

the same areas under collimated lighting at 0° (full moon) and 90° (quarter moon) phase angles, respectively. At the full-moon condition the simulated rays are noticeable, whereas at the quarter moon they are not. The photographic observations are confirmed by the relative photometric curves of the rays and of their background, as shown in figure 5(d). For the particular albedo-roughness combinations used in the experiment, the two curves nearly coincide beyond 90° phase angle. Other combinations are possible. For instance, it is conceivable that the rays may actually appear darker than their surroundings at large phase angles, if the difference in roughness outweighs, photometrically speaking, the difference in albedo. Such a condition may occur if the rays, unlike their surroundings, are rough both on a microscale and a macroscale. We have not simulated this condition in our experiment nor do we know whether it exists on the Moon.

The present proposition, based on purely photometric considerations, that the lunar rays are on the average "rougher" than their surroundings, is in accord with the commonly accepted view on the structure of the rays. The actual scale of this roughness may range from a fine, intricate microstructure, to macrofeatures such as craterlets and boulders. Although the latter features may be resolved in Orbiter photographs, knowledge of the temporal behavior of gray tones on these photographs is necessary in order to assess the microstructure and, by inference, the porosity and bulk density of the surface layer.

POLARIZATION ANOMALIES AND THEIR MEANING

The polarimetric signature of the lunar surface has distinctive characteristics which have been described earlier in this paper. It is to be expected that selected areas of the Moon will present a polarimetric signature differing substantially from the norm. On the Earth, where features such as vegetation and water break the monotony of the surface, polarimetric anomalies much stronger than those on the Moon may be expected. If the anomalous signature can be shown to be characteristic

of certain features, such as vegetation, or more specifically, certain types of vegetation (e.g., evergreen foliage), an important reconnaissance interpretation key may be evolved. On extensive lunar and planetary areas where no vegetation or areas of culture are known to exist, it may be that rather subtle differences in polarimetric response may be interpreted in terms of changes in surface texture or related physical qualities having practical importance.

Early attention to temporal data of lunar origin has led to speculation concerning the occurrence and meaning of lunar polarimetric anomalies and subsequently to application of some of this thinking to the potential value of the terrestrial anomalies. In either case, in order to interpret anomalous data one must understand the physics of the polarization phenomenon and the important factors that shape the polarimetric signature.

The polarization-inducing optical phenomena are those which are associated with boundary conditions between media of different refractive indices. These are reflection, refraction, and diffraction. The interplay of these phenomena in a surface of great complexity is not conducive to ready quantitative analysis. The shadow formation which seems largely responsible for sharp backscattering photometry further complicates lunar polarimetry.

One approach to analysis is polarimetric measurements performed on surfaces of various orders of complexity and attempts to discover generalizations which can be incorporated into a useful hypothesis. Another approach is to apply known physical laws to generalized models and to try to approach the known polarimetric signatures mathematically. We have used both methods of approach but will describe here physical measurements on one reasonably good laboratory analog of the lunar polarimetric signature and on two highly abstracted contrived surfaces.

Figure 6 shows a typical lunar polarimetric signature in terms of percent polarization as a function of phase angle. A curve is also shown representing this same kind of function as determined on the Grumman polarimetric analyzer from a sample of powdered volcanic cinder.
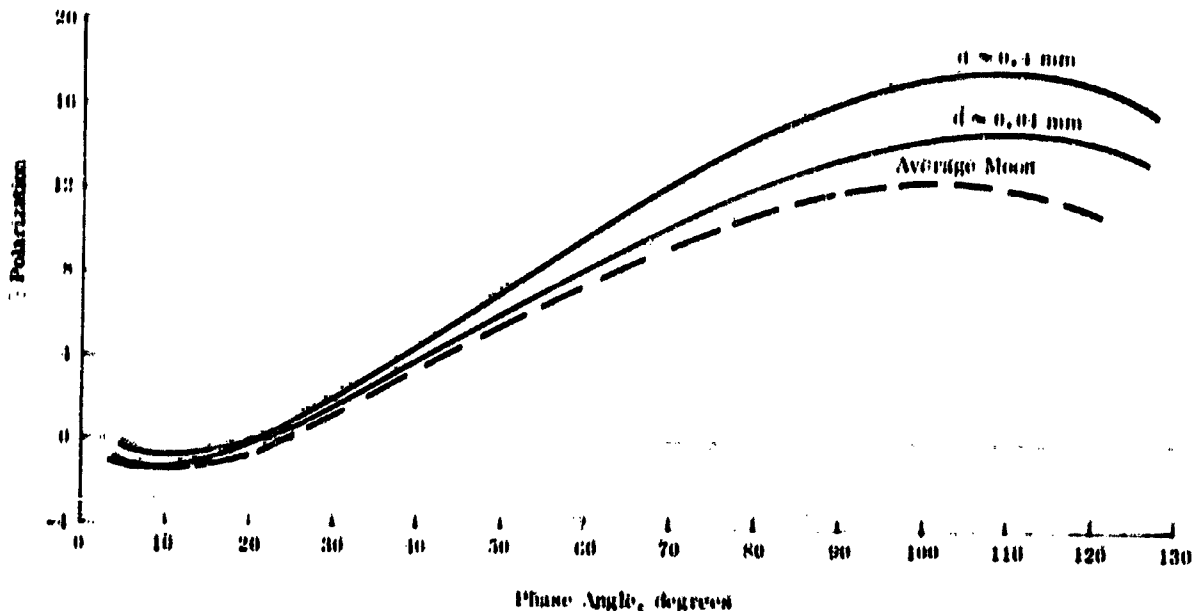
FIGURE 6.—Polarimetric signature of Hawaiian volcanic ash and Moon; d, particle size.

The features of negative yielding to positive polarization at a characteristic inversion point are present in the model, but the positive polarization at large angles is too high in the model's function.

One of the simpler approaches to analysis is to make the assumption that the complex surface can be represented by an aggregate of random reflecting plane facets inclined at various angles to the plane of vision. For practically any material the singly reflected light from a facet oriented normal to the plane of vision is positively polarized as referred to the plane of vision. If the facet is not normal to the plane of vision but is rotated about an axis in that plane, the polarization may be quite negative. An experiment is shown in figure 7(a) to clarify the point. The masonite board has a pronounced positive signature when presented as a plane surface to the polarimetric analyzer. When two reflecting facets of the masonite are formed into a V-shape and the facets are oriented normal to the plane of vision, the polarimetric signature is pronouncedly positive. When the V-shape is oriented with the vertex in the plane of vision but the facets are inclined to the normal as shown, the polarimetric signature is

quite negative at small phase angles and becomes positive only at large phase angles. This trend was anticipated when the experiment was planned because positive polarization becomes negative polarization if the coordinate frame of reference can be rotated 90°. In the signature of this model there evidently is a strong competition between the factors favoring a preponderance of light with the vector arbitrarily defined as negative and the factors favoring the vector defined as positive. The point at which this competition is equal is the inversion phase angle.

An even more striking artificial example of the positive-negative competition is afforded by the polarimetric signature of aluminum structural honeycomb shown in figure 7(b). Structural honeycomb is extremely porous and the pore lining is specular in reflecting properties. A signature secured on the polarimetric analyzer with the pores inclined very slightly to the plane of vision shows an exaggerated version of the trend mentioned above. Covering the pores with strips of cardboard results in successive steps of reduction of inversion phase angle and reduction of negative polarization, while the positive component is enhanced. The
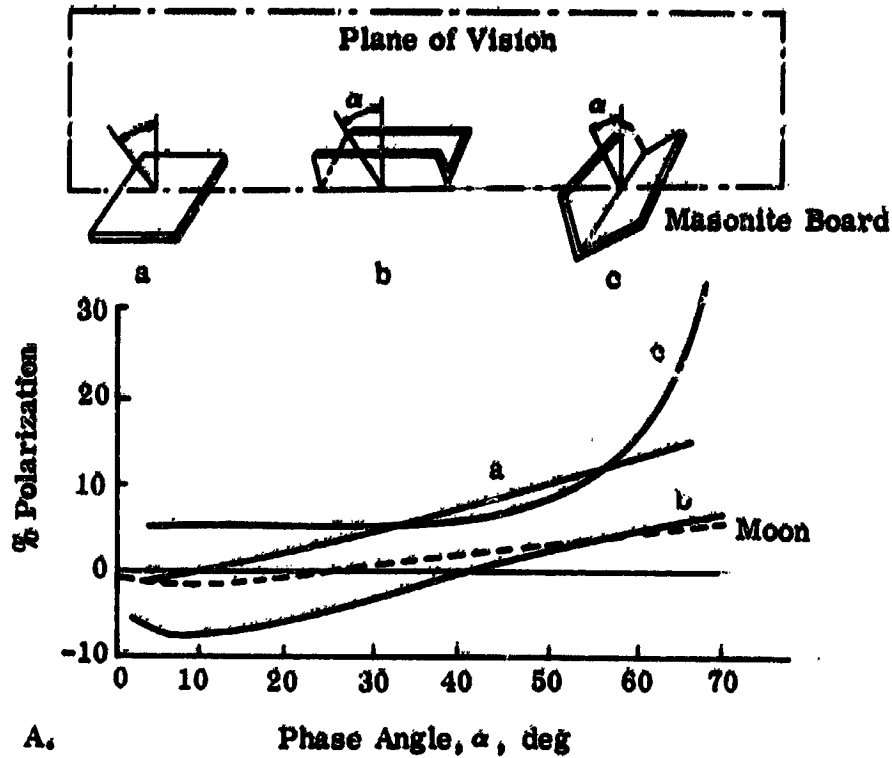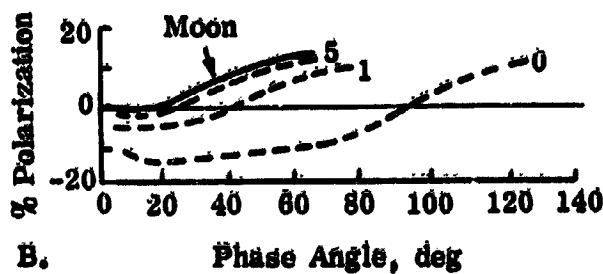
FIGURE 7.—Contrived models showing effect of structure on percent polarization. (a) Polarization by orientation of plane facets. (b) Polarization of honeycomb covered with varying number of cardboard strips. (Note change of signature with change of surface porosity.) Numbers at each curve are number of cardboard strips.

cardboard is one of the normal opaque reflecting surfaces which have a predominantly positively polarized signature.

Structural effects arising from the orientation of the facets with reference to the plane of vision are not the only mechanism inducing negative polarization. Other experiments with transparent dielectrics, such as water, have demonstrated strong contributions to negative polarization arising from refraction and subsurface reflection (ref. 12). There appears to be a connection here to the polarization signature of vegetation and the degree of turgidity, or state of hydration, of the vegetation. One example is shown in figure 8 for fresh and dehydrated vegetation.

The experiments with two contrived models described in figures 7(a) and 7(b) demonstrate that the polarimetric signature may be related to structure even on a fairly gross scale.

Neither high nor low limits on the scale of the structural grains are set, as long as attention is confined to the opaque reflecting surface facets. When semitransparent grains are considered, the grain size may be an important parameter because of increasing opacity with size. The magnitude of the refractive boundary effects which may tend to enhance negative polarization is related to grain size. This can be verified by examination of the degree of conformance of the signature of our sample of volcanic ash with that of the Moon (fig. 6).

One of the most difficult features of the lunar surface polarimetric signature to duplicate is the relatively low positive polarization at large phase angles. There are many factors related to surface structure which could be postulated to account for this feature, and it is possible to perform experiments which demonstrate trends in this direction. Multiple scattering and high

Fresh Green Dogwood
Leaves (10-11-66)

Dried Green Dogwood
Leaves (1 Week) (10-18-66)
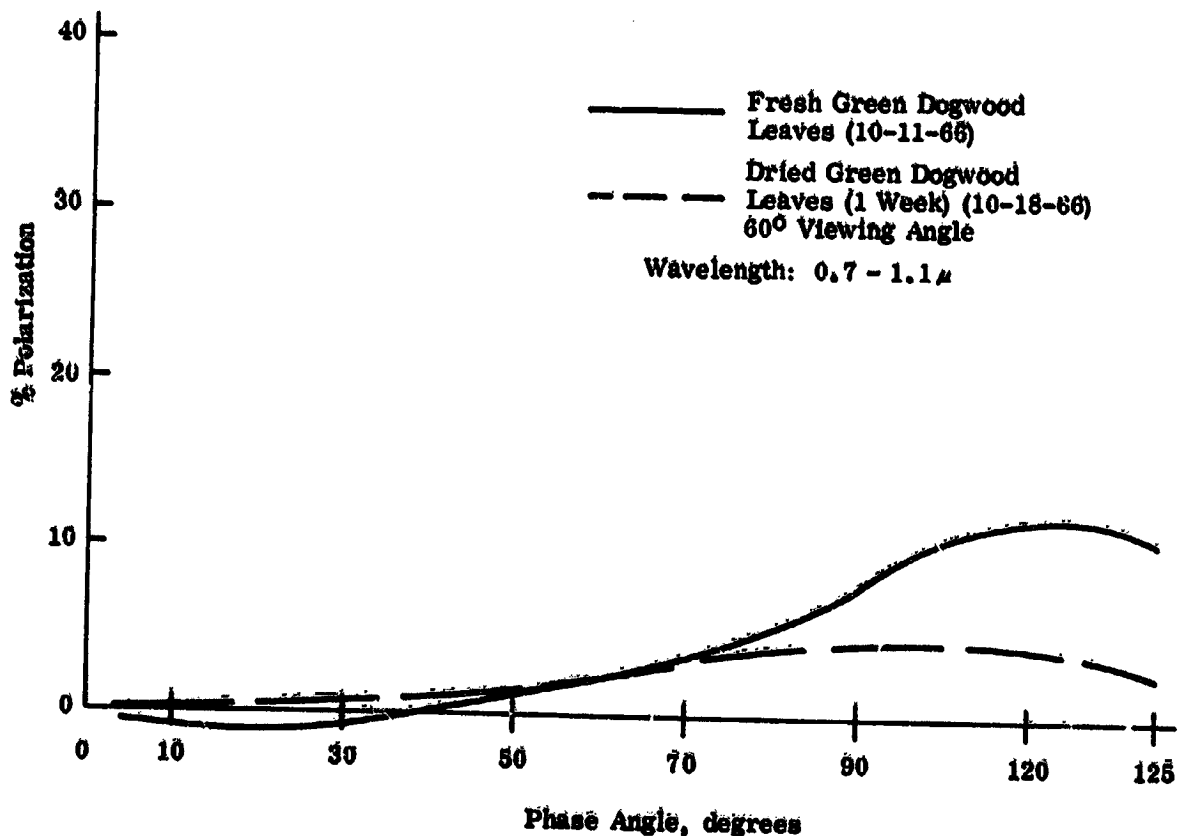60° Viewing Angle

Wavelength: 0.7 - 1.1 μ

Figure 8.—Polarization of fresh and dried vegetation at near infrared wavelength.

albedo, in general, favor depolarization. Multiple scattering combined with factors favoring the negative vector are logical assumptions in the effort to understand and duplicate the lunar signature at large phase angles. Presumably other planetary surfaces may possess the same general characteristics, thereby justifying further attention to rationalization of the lunar polarimetric behavior.

Obviously many factors operate to modify the polarimetric signature. Only in the case of rather simple surfaces is interpretation easy. As in the case of photometry, the utility for remote sensing seems to be largely to draw structural rather than compositional inferences. Also it seems clear that polarization is one of many optical phenomena that could be most meaningful when correlated with other temporal data, such as photometry, and with measurements of albedo and color. In specific instances, such as the example of vegetation mentioned, a polarimetric anomaly should lend itself quite readily to interpretation, but it is felt on the average that considerable analysis of a cross-correlation nature must be done prior to reaching a conclusion.

Inasmuch as polarization is a measurable characteristic and seems to be related to structure, and to some degree to composition, it should be a potential source of additional information. However, it is a very complex phenomenon and much remains to be learned. Certainly field polarimetry concurrent with photometry and radiometry can be justified.

USES OF TEMPORAL DATA IN INTERPRETING INFRARED THERMAL ANOMALIES

Temporal data at optical wavelengths provide, at best, information on surface properties, such as texture and roughness, but are inherently not capable of revealing bulk properties of the surface layer, such as thermal conductivity and bearing strength, unless they are supplemented by data at infrared and longer wavelengths.

Currently available temporal data on the thermal infrared emission of the lunar surface are far from adequate for a meaningful diag-

nosis. They are, however, surprisingly more extensive than their counterpart at optical wavelengths despite the difficulties inherent in measurements at the longer wavelengths.

Observations to date (refs. 6, 7, and 8), whether made during an eclipse or lunation, have been rewarding insofar as they have revealed a number of anomalies which are generally, but not always, characterized by cooling phase temperatures that are higher than their surroundings. Various hypotheses have been offered to account for the "hotspots." The most plausible among these associate the phenomena with a rough mixed dirt-rock surface (refs. 13 and 14); a more conductive, hence, harder subsurface material (ref. 15); and internal heat sources. Consequently, the problem of exploiting thermal emission in remote sensing as a clue to the nature of the lunar or any remote surface resolves to disentangling these and other relevant factors. In the case of the Moon the factors to consider are the geometrical, mechanical, thermal, and optical properties of the uppermost layer. These unknowns and the assumptions they impose on the analysis have been the main obstacles in past attempts to match lunar data with analytical solutions.

One approach that promises to reduce some of the ambiguities of the data is utilization of the fact that the thermal behavior of the lunar surface can be observed during a day, night, and eclipse cycle. Although such observations of the Moon have been made, there have been no attempts to monitor and correlate the thermal behavior of a given area during all three temporal regimes. Also, the possibility that each regime could contribute an independent equation to the solution of the various unknowns has not been adequately explored theoretically. Similar remarks can also be made in favor of lunar investigations at microwave frequencies. However, this topic will not be discussed.

The new approach could begin with analysis and end with observations. In the analytical phase, standard curves can be derived in order to describe the lunation, eclipse, and directional behavior of a homogeneous, semi-infinite, blackbody material with Lambertian elements. Call this the "zero-order model." Next, one

could upgrade this model and determine the way in which known inputs perturb its lunation, eclipse, and directional signatures. Albedo, emissivity, thermal conductivity, bulk density, particle size, vertical inhomogeneity, surface roughness, and an internal heat source are examples of such inputs. There now is sufficient knowledge to propose that the solution of the higher order models could help narrow the number of possible interpretations that have been given to the lunar thermal anomalies. Some of this knowledge is discussed briefly in quantitative terms whenever possible and qualitatively where no analyses have yet been made.

Consolidation Effects

Bearing strength is a factor for consideration in the interpretation of lunar hotspots because of the relationships that will now be described. The temperature of a cooling surface is a sensitive function of the thermal conductivity of the cooling material; both thermal conductivity and bearing strength are functions of the same physical properties, such as porosity, particle or pore size, the degree of consolidation between the solid elements, and the nature of the solid material. In a recent study by Halajian et al. (ref. 15) these properties were used as a link in order to correlate the midnight temperature of the lunar surface with the bearing strength of postulated lunar surface materials ranging from loose, fluffy powders to solid rock. The analysis was made in terms of nighttime rather than eclipse temperatures, because roughness effects (discussed below) contribute to thermal enhancement during a short cooling transient and consequently complicate the correlation of thermal and mechanical properties. The results of this study based on lunation temperatures are summarized graphically in figure 9. Notice that midnight temperatures are far more sensitive to changes in bearing strength than are noon temperatures. Very low temperatures at night (i.e., coldspots) correlate with soft powders; elevated night temperatures (i.e., hotspots) correlate with porous rocks. The fact that noon and night temperatures show opposite trends with respect to bearing strength should be of diagnostic value and will be discussed later. Figure 9 also shows

the bearing strength and day and night temperatures of the Surveyor I landing site. The concurrence of these data with the theoretical curves is quite good.

Roughness Effects

Surface roughness, neglected in the above analysis, is another important factor to consider when one is interpreting thermal emission. Day, night, and eclipse temperatures could be influenced by roughness to an extent and for reasons that differ in each case. These effects are extremely complex and interact with others that are no less complicated. An oversimplified view of the problem is taken here with the hope of identifying areas that deserve close scrutiny.

To begin with the insolation phase, roughness can affect daytime temperatures in two different ways. One is by shadowing which tends to lower the effective temperature and the other is the directionality (of the randomly oriented planes) which tends to raise it. Both effects are pronounced at oblique viewing (i.e., toward the limbs when the Moon is observed from the earth), but fortunately they do not occur simultaneously. Obviously, shadowing effects are most pronounced at large phase angles (during the first and last quarters) but directional effects take place mostly at small phase angles (at or near full moon) because the viewing angle gives more weight to those slopes whose normals are oriented toward the same direction is the incident solar radiation.

Figures 10(a) and 10(b) illustrate the way in which directional and shadowing effects could respectively enhance or attenuate thermal emission, the variation depending on the phase angle. In our opinion, these effects produce the anomalous temperature variation of the Surveyor landing site shown in figure 10(c) (ref. 16). Expressed in graphical terms, roughness tends to skew the overall lunation curve toward the viewer, when the viewing is at oblique angles. This skewing effect should not be surprising since its existence at optical wavelengths is widely recognized. It is tempting to think that its persistence at infrared wavelengths could be exploited as a clue to surface roughness at a scale larger than the
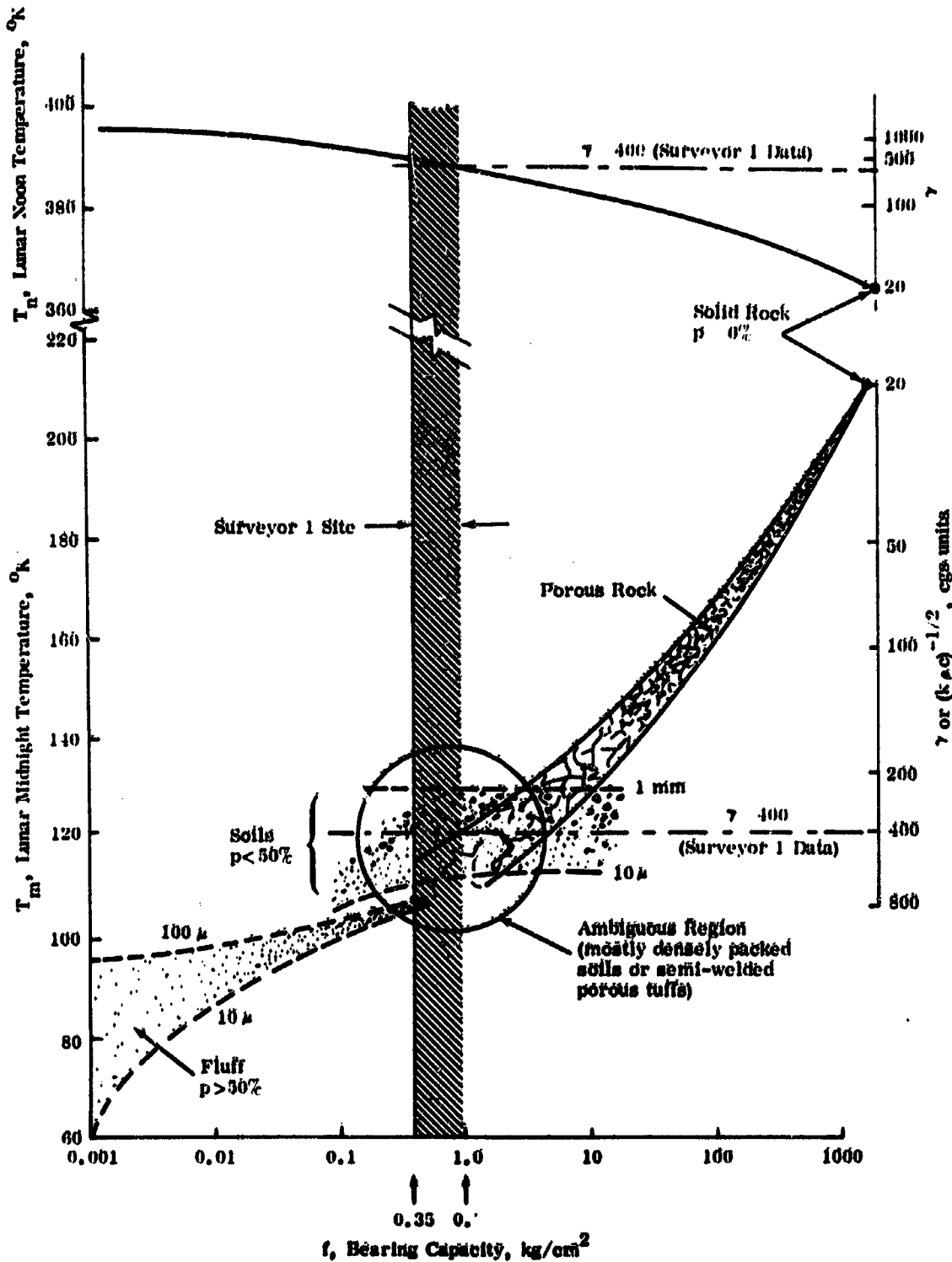
FIGURE 9.—Correlation of lunar temperatures and bearing strength; p, porosity, percent; γ, thermal inertia constant.
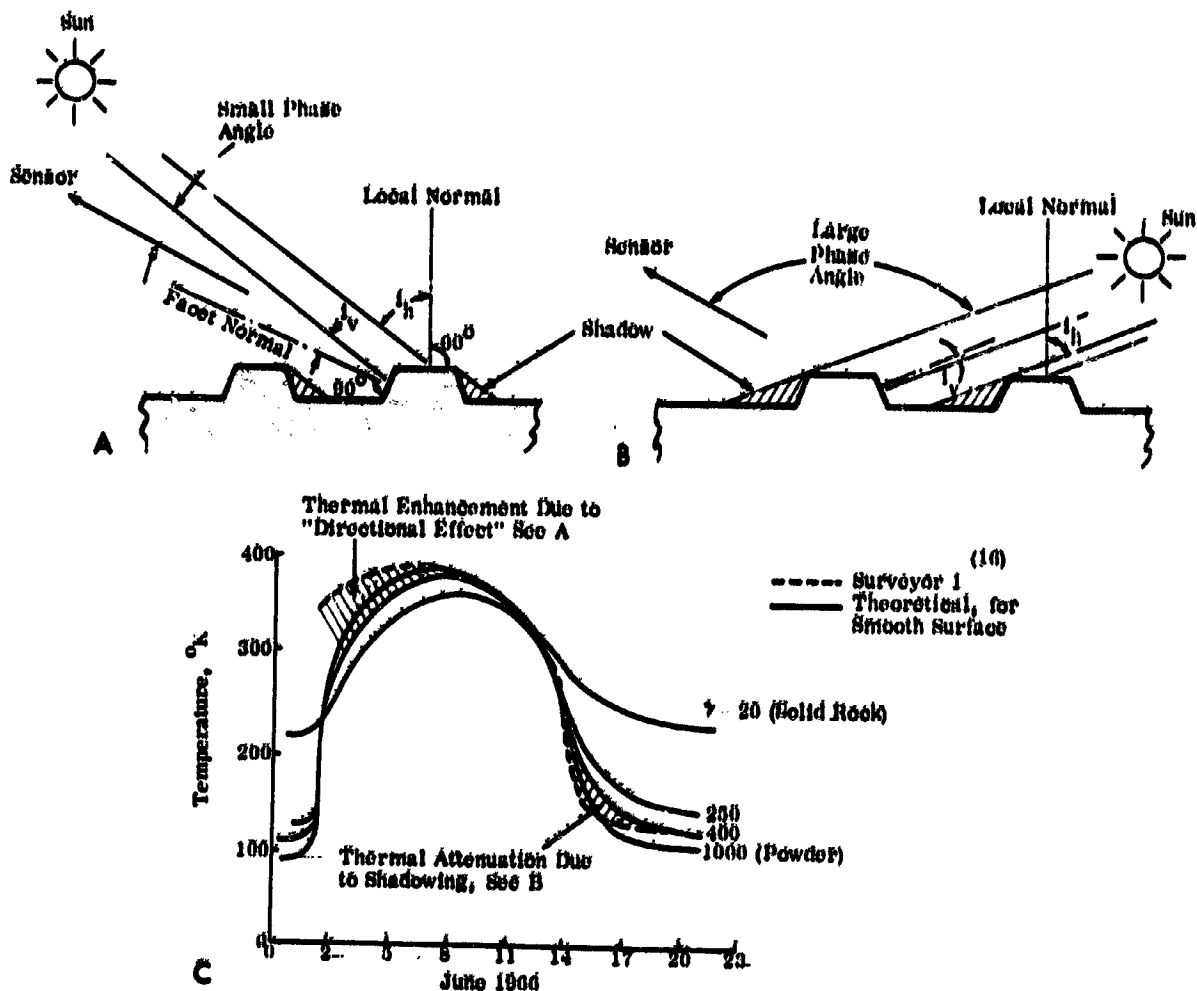
Figure 10.—Mechanisms of daytime thermal enhancement and attenuation caused by roughness; diagnosis of Surveyor I data.

(a) Directional effect at small phase angles. Observed average temperature is more than temperature predicted for smooth surface because thermally enhanced facets (where $f_v < f_h$) are seen by sensors but shadows are not.

(b) Shadowing effect at large phase angles. Observed average temperature is less than temperature predicted for smooth surface because thermally enhanced facets (where $f_v < f_h$) are not seen by sensor but shadows are.

(c) Family of theoretical lunation curves and curve for Surveyor I landing site.

microstructure. Thus, a rough area will appear cooler at large phase angles and warmer at small phase angles than will a smooth area, other parameters being equal. The most important of these parameters are albedo, emissivity, and the thermal inertia constant commonly designated as γ. The latter parameter is closely related to hardness or degree of consolidation. Albedo and emissivity could be estimated by using multispectral measurements, but γ must be assumed.

A family of theoretical lunation curves as a function of γ is shown in figure 10(c). It previously has been noted that γ does not affect the temperatures at the small phase angles (where directional effects take place) as much as it affects the nighttime temperatures. Notice also that at the large-phase-angle portion of the daytime curve (where shadowing effects are most pronounced) the temperatures are nearly insensitive to wide variations of γ. It appears therefore that thermal emission at

large phase angles also is a clue to roughness; this could verify or supplement the roughness inferred from photographic, photometric, radar, and other sources.

Considerations of the scale of roughness that is thermally relevant lead to similar conclusions. The "microshadows" which are formed mostly at the small phase angles are not likely to be thermally as significant as they are at optical wavelengths. During the long lunar day, the small shadows in the recesses of the microstructure progress at a rate slower than that at which heat is transferred into these areas through lateral conduction and radiation. Therefore, the microshadows will be in near thermal equilibrium with their sunlit surroundings. Accordingly, the lunar surface which is known to be rough at optical wavelengths should be relatively smoother at far-infrared wavelengths. In figures 2(a) and 2(d), a comparison of the sharp backscatter peak of the photometric curve with the convex curvature of the thermal infrared curve supports this view.

If roughness is to have a measurable effect on daytime thermal emissions, it should be at a scale sufficiently large to produce long shadows that remain cooler than their surroundings. In lieu of an actual analysis, one can only speculate that topographic features, including those that are below the resolution of the viewing systems, could cast shadows of this magnitude at large phase angles and reduce the average thermal emission below that predicted for a smooth surface. Thus measurement of lunar temperatures during the early morning and late afternoon periods may have a diagnostic value in terms of roughness that has not been exploited, probably because this possibility is not apparent in the well-known γ-dependent lunation temperature curves in figure 10(a). The fact that thermal behavior during these periods is nearly independent of γ should make the interpretation of the data in terms of roughness less ambiguous than it usually is.

Next, consider roughness effects on dark-side temperatures. Roughness will enhance thermal emission during night or eclipse cooling to an extent that is inversely proportional to the duration of the cooling transient. Again, every-thing else being equal, a rough surface will appear warmer than its smoother surroundings, essentially because its component facets radiate to a value of less than 2π steradians and hence require a longer cooling period than a smooth surface which radiates its heat to a full hemisphere. Unfortunately, the fact that consolidation effects and internal heating also could contribute to thermal enhancement during a cooling phase complicates but does not necessarily obscure the interpretation of lunar hotspots. We suggest the following technique for disentangling the contribution of roughness and internal heating to thermal enhancement observed during the night or an eclipse.

In the first place, one can take advantage of the fact that thermal enhancement caused by roughness, unlike that caused by the other two factors, is of temporary duration. A long cooling transient effectively acts as a time filter during which roughness-induced hotspots fade away and leave those that are caused by internal heating and/or a thermally more conductive, hence, harder, material. Thus, with a sufficiently long cooling period, such as that during the lunar night, a rough and a smooth area of similar thermal and mechanical properties should reach about the same predawn temperature. Interpretation of thermal enhancement during an eclipse would be more ambiguous than would be that of thermal enhancement during the night because it could be caused by any one, or a combination, of the three factors mentioned above. Roughness could be suspected as a primary or unique cause of thermal enhancement during an eclipse only when this enhancement does not persist at night. The converse situation, where an area is thermally enhanced at night but not during an eclipse, is possible in the case of weak anomalies which can be detected only at very low temperatures. In such a case roughness (up to a certain scale than can be estimated) could be eliminated and the interpretation can be narrowed to the other two factors. A similar interpretation may be given to the strong anomalies that are prominent during both the night and eclipse.

A recent quantitative analysis of roughness effects on lunation and eclipse cooling by Staley (ref. 17) and Roelof (ref. 14) support

some of these views. Staley estimates that most thermal enhancement in craters observed during eclipse by Shorthill and Saari (ref. 8) can be accounted for in terms of radiative interchange between the crater walls. Roelof reports that during eclipse rocks smaller than a meter in diameter can produce small but detectable variations in Earth-based measurements, but during the night the size of the rocks should be larger than a meter in order that there be a similar effect. He estimates a thermal enhancement of about 3° K during midnight for a typical lunar surface, 1 percent of which is occupied by 3-meter rocks. He points out that this is far more negligible than the value previously estimated by Hopfield (ref. 13). However, he remarks that such rocks could produce strong thermal enhancement in local measurements, such as those made by Surveyor, particularly at sunrise or sunset when the Sun and sensor are on the same side of the local normal. It seems reasonable therefore to neglect roughness as a factor in remotely observed thermal enhancement during the lunar night unless Orbiter photographs and photometric data (if available) indicate otherwise.

As to the other hypothesis (that daytime thermal emission at large phase angles could provide clues to unresolved topographic roughness), it remains to be substantiated by analyses and observations.

Internal Heat Sources

Certainly, the discovery of internal heat sources on the Moon would be of major scientific and engineering significance. The question arises, therefore, whether these sources can be detected by remote means and, if so, whether they can be positively identified as such.

The problem of identification, in the case of the Moon, narrows to being able to discriminate between "geothermal" and "structural" effects since, as we have seen, both effects could contribute to thermal enhancement during the night or eclipse. We focus attention on nighttime temperatures, because they are less subject to roughness effects than are eclipse temperatures and are more likely to reveal weak anomalies that may not be otherwise detected. However, nighttime measurements are not sufficient for a unique identification of the hotspots unless they are supplemented by daytime data. This proposition once more affords an opportunity to stress the importance of temporal data.

We assume for the purpose of this discussion that an internal heat source is detectable, that is, that it is sufficiently strong to have a measurable effect on a remote sensor over and above the thermal emission of the surface because of normal insolation. If this is the case, then it is possible to discriminate between the solar and nonsolar components of the observed emission by balancing the heat budget of the anomaly for a complete day and night cycle. Notice in figures 9 and 10(e) that the "hardness" parameter γ perturbs the midnight temperature T_m and the high-noon temperature T_h in opposite directions (T_m increases and T_h decreases with decreasing γ), but an internal heat source would push both day and night temperatures in the same direction (up). Thus, if T_m and T_h are known and the latter is found to exceed the theoretical value predicted by solar input, albedo, emissivity, and T_m, then a nonsolar heat source must be postulated in order to balance the heat budget.

The above concept may be expressed graphically in terms of the area under the curve that represents the thermal-infrared emission during a complete diurnal cycle. This area is independent of the hardness and roughness parameters. In the absence of nonsolar heat and negligible lateral heat losses, it is solely a function of the hemispheric albedo of the surface and the incident solar energy. If it is assumed that the radiated energy is uniform over a hemisphere and albedo differences are accounted for, then processing the data in terms of the area under the lunation curve may be a convenient way of identifying the anomaly. If the index area of the anomaly is more than that of the surrounding region or of the value predicted by solar input, then an internal heat source may be suspected.

The basaltic composition of the maria, as analyzed by Surveyors 5 and 6, suggests that

differentiation, probably caused by internal sources of heat, has occurred on the Moon. To date, none of the known thermal anomalies of the Moon have been positively identified as internally hot; this is primarily because of the lack of accurate data on the diurnal behavior of these anomalies, it is believed.

A summary of our thoughts on the nature and meaning of lunar thermal anomalies is presented in table 1. The summary is necessarily oversimplified and is meant to stress major trends in temporal signatures and the supplementary nature of the thermal data during a day, night, and eclipse cycle.

CROSS-CORRELATION OF LUNAR TEM. PORAL DATA AT OPTICAL AND INFRARED WAVELENGTHS
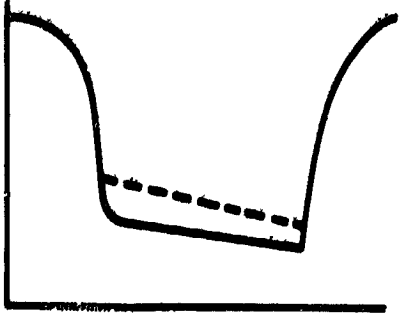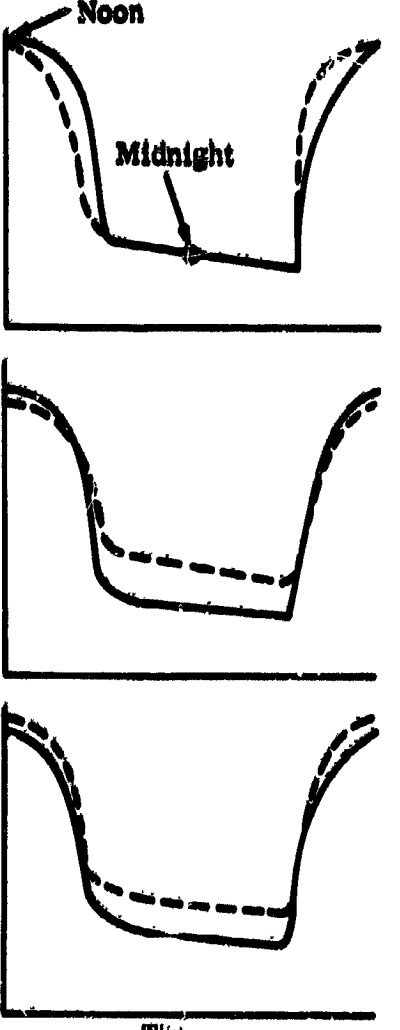
The selection of suitable lunar landing sites (suitable from a smoothness and hardness point of view) is discussed here as a case in point to illustrate how temporal data at optical and infrared wavelengths could supplement purely pictorial information including those data recently obtained with the highly successful Lunar Orbiters. We recall how the criteria of smoothness and hardness in the case of the Moon could be correlated, as a first approximation, with the area under the normalized photometric curve and the midnight temperature, respectively. We submit now that accurate measurements of the optical reflections and thermal-infrared emission of the lunar surface during a full lunation, and the computer processing of these data in terms of the above indices, make it possible to rate in a quantitative and objective manner the relative smoothness and hardness of any number of potential landing sites approaching in size the resolution of the viewing system. In Earth-based lunar observations, this resolution can be approximately as fine as a kilometer at optical wavelengths and about 5 to 10 times coarser at infrared wavelengths.

This concept is illustrated in figure 11. The ordinate of the chart, designated as the "optical index," represents the area under the normalized photometric curve and is a direct measure of smoothness as shown in figures 3

and 4. The abscissa, designated as the "thermal-infrared index," represents the midnight temperature and is a direct measure of hardness or bearing strength as shown in figure 9. The data points in the chart represent potential landing sites of known selenographic coordinates selected either at random or from Orbiter photographs. For purposes of discussion, the diagram is arbitrarily divided into four quadrants numbered from 1 to 4 and labeled as soft-rough, soft-smooth, hard-smooth, and hard-rough, respectively. Soft-rough regions are not likely to exist on the Moon as they would be most closely approximated, in our opinion, by forest treetops. A surface of this nature is likely to be optically and thermally subdued at the diagnostic phase angles. In other words, it will appear dark during the day when viewed in the specular direction (i.e., against the Sun) and cold at night. Most lunar areas, including the Surveyor landing sites, are likely to crowd around the center of the diagram, and the anomalies would fall toward the outer edges. Photometric anomalies will occupy the extreme ends of the ordinate, the good (i.e., smooth) anomalies falling in quadrants 2 and 3. Thermal anomalies will occupy the extreme ends of the abscissa, the good (i.e., hard) anomalies falling in quadrants 3 and 4. Consequently, quadrant 3 will be the locus of the best anomalies from the point of view of landing-site selection. These are the areas that are optically enhanced during the day and thermally enhanced during the night.

The classification and pairing of optical and thermal anomalies need not be limited to a few areas of interest, such as those selected from Orbiter photographs. In general, diagnostic indices (such as the coordinates of fig. 11) make it possible to use the computer in processing a vast number of data points, where each point could represent an element of resolution. It should be cautioned that these indices are rarely unambiguous. However, their use in computer processing can be justified as a means of discovering rather than identifying the anomalies. Numerous potential landing sites or prime targets of exploration that may not be otherwise discovered could be located in this

TABLE 1.—*Summary of the Nature and Meaning of Lunar Thermal Anomalies*

Cycle	Temporal signature [a]	Possible clue to—	Comparison index [b]
Eclipse		Roughness Hardness Internal heat (Ambiguous)	Anomaly—warmer during eclipse
Lunation		Roughness	1. Anomaly at oblique viewing is skewed toward small phase angles 2. $A_a = A_b$
		Hardness	1. Anomaly—warmer at night and colder at noon 2. $A_a = A_b$
		Internal heat	1. Anomaly—always warmer 2. $A_a > A_b$

[a] Dotted curve is the anomaly; solid curve is region surrounding anomaly.
[b] A, area under curve; subscripts a and b, anomaly and its surroundings, respectively.

"Best" lunar anomalies (in terms of landing
suitability) will fall in this quadrant ⟶

Optical index, (area under photometric curve)
Increasing Smoothness ⟶

② Soft & Smooth
(Dust Bowls)

③ Hard & Smooth
(Pumice Flats)

① Soft & Rough
(Forest Treetops)

④ Hard & Rough
(Lava Fields)

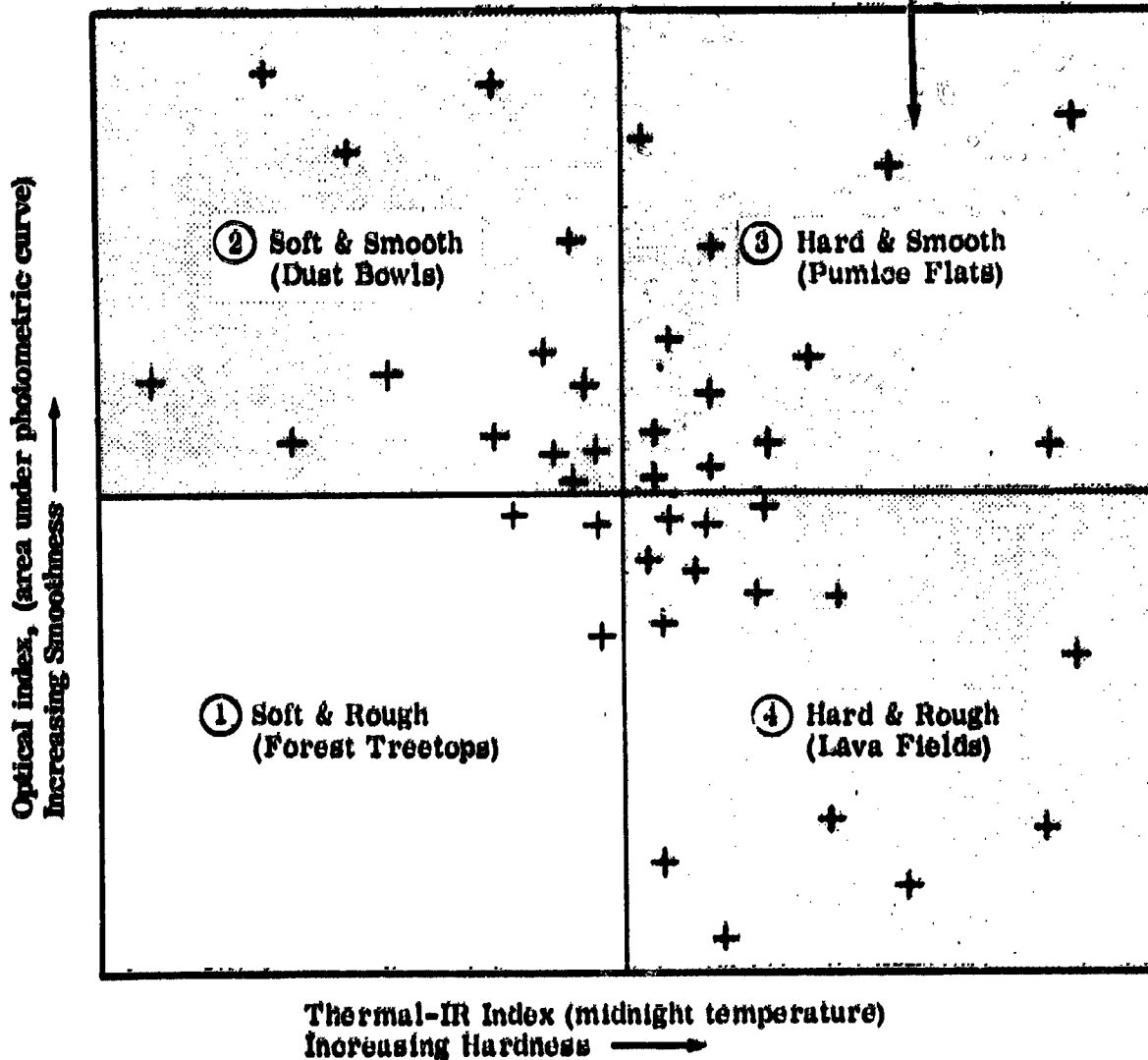Thermal-IR Index (midnight temperature)
Increasing Hardness ⟶

FIGURE 11.—Sorting of lunar photometric and thermal anomalies in terms of correlated terrain smoothness and
hardness. Crosses represent investigated areas defined by their selenological coordinates.

manner. Identification could then follow, the
process beginning with an examination of the
most pronounced anomalies. This process will
involve a detailed analysis of the shape and
local peculiarities of individual temporal curves.
As previously discussed, this analysis could
disentangle the contributions of microroughness

and macroroughness to the photometric func-
tion and the contribution of geometrical,
structural, and geothermal factors to the
radiometric function. This step could also be
automated but only up to a certain point
beyond which the interpreter should exercise
his judgment.

A CASE FOR EARTH-BASED OBSERVATION OF THE MOON

There is currently a justified optimism on the lunar landing phase of the Apollo mission because of the remarkable success of the Surveyor and Orbiter missions. However, these successes should not obscure the fact that Earth-based observations of the Moon can fill certain specific gaps in our knowledge that were not meant to be explored by these probes. Properties of the lunar surface that can be correlated with temporal observations are examples of such gaps. While temporal data on the Moon can be extracted from thermal measurements and sequential photographs taken by Surveyor craft, such data are limited to the landing sites and can, at best, be used as calibration points for remote, synoptic observations. Orbiter photographs are synoptic in coverage but are presently limited in their spectral and temporal ranges. Earth-based observations of the apparent lunar disk can extend these ranges, although at some loss in spatial resolution. However, the potential of extracting information on surface porosity, subresolution topographic roughness, bearing strength, internal heat sources, and material composition will more than compensate, in our opinion, the loss in resolution.

Ironically, the advent of lunar exploration by manned and unmanned probes is one reason such extensive observations of the Moon have not been made. An equally important reason is that the quantity and quality of the data needed to justify new observations impose severe problems in instrumentation and data processing. For instance, photometric observations are fraught with difficulties of light calibration and film processing when the photographic method is used. More accurate data can be secured by using photocells but at a sacrifice in the quantity and resolution of the data. However, recent advances in image tube technology and digital data processing make it possible to chart the photometry, polarimetry, and spectral reflectance of the apparent lunar disk at a resolution approaching that of conventional lunar photographs and with a gray tone and color fidelity superior to

that of these photographs. As to the thermal-infrared emission of the lunar surface, its measurement during the lunar night has been hampered by the limitation of existing sensors to detect temperatures lower than about 100° K. However, progress in this area has been reported by Low (ref. 7), who developed a helium-cooled germanium bolometer capable of measuring these temperatures.

These advances in sensor technology and the availability of ground truth information secured by the Surveyor and Orbiter probes offer the opportunity to verify and refine laboratory-inspired techniques of interpreting lunar pictorial, spectral, and temporal data. Progress in remote sensing, as in other fields of science, will come through continuous feedback between observation and theory. There are cogent reasons why the study of the Moon should be a first step in this particular exercise. The Moon is a more convenient target for temporal observations than is any other object in the sky by virtue of its proximity to and phase relationship with the Earth. Furthermore, the analysis of its optical reflection and thermal-infrared emission is not complicated by convective air currents, ground moisture, and a vegetation or cloud cover, as is usually the case for the Earth and possibly for most other planets. As a proving ground for the subsequent exploration of the planets by remote means, the Moon offers many advantages for developing techniques of data collection and interpretation. Certainly there is no valid reason for doing any observation in space that can be accomplished adequately on the ground.

CONCLUSIONS

We have defined "temporal data" as the repetitive, sequential measurement of electromagnetic radiation from a planetary surface during a periodic cycle and found that these data can be correlated with terrain properties that cannot be readily inferred from pictorial or spectral data.

Information on unresolved structure is the most important payoff resulting from temporal data at optical wavelengths. It can now be reported that both subresolution roughness and micro-

structures beyond the resolution of the viewing system are important contributions to the standard lunar photometric function and that they can be discriminated by photometric means. Experiments clearly show that the two scales of roughness perturb the leading edge (i.e., opposition region) and the tail end of the photometric curve independently of each other. They also suggest that improvement in spatial resolution could lead to the discovery of lunar photometric anomalies and to a thematic mapping of the lunar surface in terms of its microstructure and topographic roughness.

The percent polarization-versus-time curve at visible wavelengths appears also to be a function of structure, whether the surface is vegetative or mineral, but it is much less understood.

Temporal data on thermal infrared emission during a heating and cooling cycle appear to be very rewarding but more difficult to measure and interpret. In the case of the Moon, it is well recognized that a number of factors, such as surface roughness, degree of consolidation (i.e., bearing strength), and internal heat sources, could contribute to and hence obscure the meaning of these data. However, our analysis shows that nighttime thermal emissions are less ambiguous (although more difficult to measure) than those during an eclipse. When nighttime temperatures are supplemented by daytime data, it appears theoretically possible to disentangle the contribution of the relevant factors. These possibilities suggest that accurate measurements and proper analysis of the thermal infrared emission of the lunar surface during a complete day-and-night cycle could lead to the discovery of suitable landing sites and geothermal heat sources.

One last point should be explained regarding the logistics of acquiring temporal data, particularly from an Orbiter. Temporal observations in the field need not consist, as we have tacitly implied throughout this report, of repetitive measurements made at relatively close intervals of time, such as those made in the laboratory. Model-matching studies indicate that a considerable saving in the quantity of data could be accomplished, without appreciable loss of information, by limiting the

field observations to a few specific Sun and viewing angles. For instance, the critical diagnostic moments during photometric observations occur at oblique viewing (say, at 60° off the local vertical) when the Sun is (1) in opposition, (2) a few degrees past opposition in the direction of the local vertical, and (3) in the specular direction. A fourth intermediate point at high noon is desirable but is not necessary. The ratio of the brightness at points (1) and (2) is a measure of textural complexity or surface porosity. (Large features as such have no effect on this ratio unless, of course, their microstructure differs from that of their surroundings.) The ratio of points (1) and (3) is a sensitive clue to macrostructure or topographic roughness. Similarly, at far-infrared wavelengths, the critical measurements are those made at high noon and midnight. While midnight temperatures are sufficient to reveal thermal anomalies, data on albedo, emissivity, and noon temperatures are necessary to identify the anomaly in terms of geophysical and geothermal factors. These considerations suggest a polar, Sun-synchronous orbit around the Moon as the most suitable for infrared observations. The complete lunation curve serves only to refine these estimates and provide additional clues to surface structure when the viewing is at oblique angles.

The usefulness of temporal data coupled with recent advances in sensor and computer technologies justify, in our opinion, renewed telescopic observations of the Moon as a source of information for lunar mission planning and possibly as a prelude to similar measurements from space.

REFERENCES

1. ADAMS, J. B.: Lunar Surface Composition and Particle Size: Implications of Laboratory and Lunar Spectral Reflectance Data. J. Geophys. Res., vol. 72, 1967, pp. 5715–5720.
2. IRVIN, N. A., JR.; AND TOBIN, M.: Spectral Measurements from 1.6 μ to 5.4 μ of Natural Surfaces and Clouds. Appl. Opt., vol. 6, 1967, pp. 1399–1402.
3. LYON, R. J. P.: Evaluation of Infrared Spectrophotometry for Compositional Analysis of Lunar and Planetary Soils. NASA CR 100, 1964.

ing and Photometric Relief of the Lunar Surface. NASA TT F-74, 1962.

5. LYOT, B.: Research on the Polarization of Light From Planets and From Some Terrestrial Substances. NASA TT F-187, 1964.

6. PETTIT, E.; AND NICHOLSON, S. B.: Lunar Radiation and Temperatures. Astrophys. J., vol. 71, 1930, p. 102.

7. LOW, F.: Lunar Nighttime Temperature Measured at 20 Microns. Astrophys. J., vol. 142, 1965, p. 806.

8. SHORTHILL, R. W.; AND SAARI, T. M.: Non-Uniform Cooling of the Eclipsed Moon. A Listing of Thirty Anomalies. Science, vol. 150, 1965, pp. 211–212.

9. HALAJIAN, J. D.: Photometric Investigation of Simulated Lunar Surfaces. J. Astronaut. Sci., vol. XIV, no. 1, 1967, pp. 1–12.

10. GEHRELS, T.; COFFEEN, T.; AND OWINGS, D.: Wavelength Dependence of Polarization of the Lunar Surface. Astron. J., vol. 69, no. 10, 1964.

11. HALAJIAN, J. D.: Albedo and Photometry of Sur-

voyor Footprints. Grumman Rept. No. AS 424–5, Grumman Aircraft Eng. Corp., 1968.

12. HALLOCK, H. B.; AND GRUZUSKAS, J.: Polarimetric Signature of Natural Water Surfaces, J. Opt. Soc. Am., vol. 57, no. 4, Paper FE12, 1967.

13. HOFFIELD, J. J.: Lunar Temperatures. T.G. No. 26, Tycho Group, Univ. of Minnesota, 1968.

14. ROSLOF, E. C.: Thermal Behavior of Rocks on the Lunar Surface. Boeing Sci. Res. Lab. Rept. 01-82-0641, Boeing Co., 1967.

15. HALAJIAN, J. D.; REICHMAN, J.; AND KARAFIATH, L. L.: Correlation of Mechanical and Thermal Properties of Extraterrestrial Materials. Grumman Res. Dept. Rept. No. RE-280, Grumman Aircraft Eng. Corp., 1967.

16. LUCAS, J. W.; CONEL, J. E.; AND HAGEMEYER, W. A.: Lunar Surface Thermal Characteristics from Surveyor 1. J. Geophys. Res., vol. 72, no. 2, 1967, pp. 779–789.

17. STALEY, D. O.: Radiative Enhancement of Lunar Hot Spots During Eclipse. J. Geophys. Res., vol. 73, no. 6, 1968, pp. 2049–2055.